# Multidimensional-constrained Suspect Screening of Hydrophobic Chemicals Using Gas Chromatography-Atmospheric Pressure Chemical Ionization-Ion Mobility-Mass Spectrometry

Xiaodi Shi[1]*, Anna Sobek[1], Jonathan P. Benskin[1]

[1.] Department of Environmental Science, Stockholm University, Stockholm 10691, Sweden

*Address correspondence to Xiaodi Shi: Department of Environmental Science, Stockholm University, Stockholm 10691, Sweden. Telephone: +46-073 891 2864. E-mail: xiaodi.shi@aces.su.se. ORCID: 0009-0008-4062-4009

13 **GRAPHICAL ABSTRACT:**

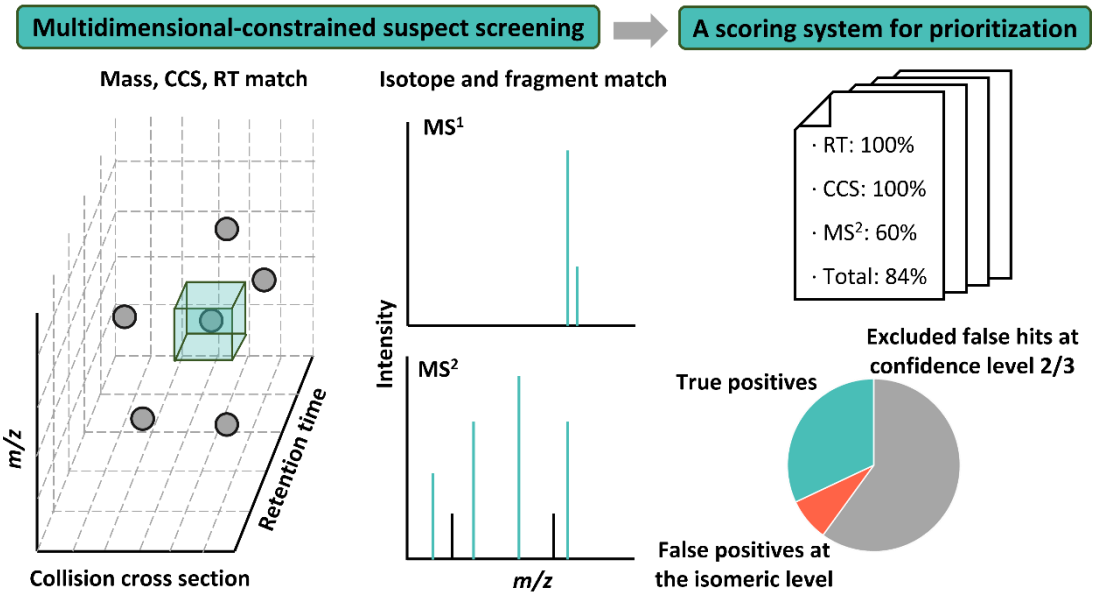


14

**ABSTRACT:**

Suspect screening strives to rapidly monitor a large number of substances in a sample using mass spectral libraries. For hydrophobic organic chemicals (HOCs), these libraries are primarily based on electron ionization mass spectra. To improve the efficacy of suspect screening, new libraries and workflows are required, leveraging the highly specific analytical data acquired by state-of-the-art mass spectrometers. In this study, we established a new library for 1,590 suspect contaminants, including exact mass and a combination of measured and model-predicted values for retention time (RT) and collision cross section (CCS). The accuracy of *in silico* predictions was assessed using standards for 102 environmental contaminants. Thereafter, using gas chromatography-atmospheric pressure chemical ionization-ion mobility-mass spectrometry, a suspect screening workflow constrained by full scan mass spectrum (i.e., $MS^1$), RT, CCS, and fragmentation spectrum (i.e., $MS^2$), together with a continuous scoring system, was established to reduce false positives and improve identification confidence. Application of the method to fortified and standard reference sediment samples demonstrated true positive rates of 79% and 64%, respectively, with all false positives attributed to suspect isomers, indicating that the method is highly specific. This study offers a new workflow for improved suspect screening of HOCs using multidimensional information, and highlights the need to enrich CCS databases and extend the applicable chemical space of current *in silico* tools to non-polar substances.

**SYNOPSIS:** A multidimensional-constrained suspect analysis of hydrophobic

chemicals was developed using gas chromatography-atmospheric pressure chemical ionization coupled to ion mobility-mass spectrometry.

**KEYWORDS:** Suspect screening; Ion mobility; Collision cross section; Hydrophobic chemicals; Sediment

## INTRODUCTION

The number of chemicals used in society is large and constantly increasing. For instance, a survey of 22 chemical inventories from 19 countries revealed over 350,000 registered substances,[1] while between 700 and 1,700 new chemicals are added each year to the United States' TSCA (Toxic Substances Control Act) and European REACH (Registration, Evaluation, Authorization and Restriction of Chemicals) inventories alone.[2] This situation challenges our capacity for chemical monitoring and risk assessment using conventional approaches. To address this issue, suspect screening has emerged as a tool for rapidly detecting a large number of substances by matching data acquired by high-resolution mass spectrometry (HRMS) to that contained in a database. High-confidence matches guide the acquisition of standards for the final confirmation or exclusion of the identification.[3]

Typically, suspect screening of hydrophobic organic chemicals (HOCs) involves matching retention indices (RI) and mass spectral fingerprints derived from gas chromatography (GC) with electron ionization (EI) at 70 eV.[4] However, this strategy is limited by the availability of EI mass spectra (particularly high-resolution) in libraries.[3,5] Further, the extensive fragmentation and frequent absence of molecular ions using EI hinder structure predictions. Therefore, novel suspect lists and workflows with high specificity using state-of-the-art mass spectrometry are required.

As a soft ionization technique for GC, atmospheric pressure chemical ionization (APCI) can harness molecular ions for HOCs through charge/proton transfer.[6] When coupled to ion mobility (IM)-HRMS, ions are further separated based on their

interactions with neutral buffering gases under an electric field. Differences in drift time produced from IM enhance the resolving-power of product ion scans by removing co-eluting ions. Collision cross section (CCS) values derived from drift times are a novel instrument-independent property of ions for identification.[7] Consequently, multidimensional information can be acquired or predicted for each compound, namely full scan mass spectrum (i.e., $MS^1$), retention time (RT), CCS, and fragmentation spectrum (i.e., $MS^2$), thereby improving the confidence in structure assignments. However, suspect screening of HOCs using multidimensional information has not been fully explored, with the exception of a few studies focused on establishing CCS databases.[7]

This study aims to establish and validate a multidimensional-constrained workflow for suspect screening of HOCs using GC-APCI-IM-HRMS. Suspect lists were compiled consisting of exact mass and a combination of measured and model-predicted RT and CCS values. A continuous scoring system was established to narrow down the number of candidates using continuous similarity information. Finally, our method was validated using sediment samples, considering their complex matrix and function as a sink for HOCs.

## MATERIALS AND METHODS

**Instrumental analysis.** The present work employed a Waters quadrupole-cyclic ion mobility-time-of-flight mass spectrometer (Waters Corp., Wilmslow, U.K.) coupled to an Agilent 8890 GC (Agilent Technologies, Santa Clara, CA, U.S.A) via APCI in

positive mode under both dry and wet conditions using previously optimized parameters.[8] The detector was operated in high-definition $MS^E$ mode with the collision energy fixed at 6 eV in low energy mode and ramped between 15-50 eV in high energy mode. The detailed instrumental method is described in Section A of the Supporting Information (SI). Progenesis QI (version 3.0, Waters Corp.) was used for lockmass correction, precursor and product ion pairing, peak picking, and alignment. $MS^1$ and $MS^2$ data were exported separately and $MS^2$ data was converted to SIRIUS format using a custom R script (available at https://github.com/Xiaodi-Shi/4D-suspect). Further information on software parameters is provided in Sections B of the SI.

**Suspect lists.** We compiled two suspect lists containing information on identity (i.e., CAS, InChIKey, and formula), exact mass, RT, and CCS. The first list was derived from matching contaminants from all GC-based suspect lists in the NORMAN-SLE[9] with experimentally-derived CCS values from a unified database of 23 scientific articles published between 2016 and 2022,[7] resulting in 1,060 compounds. A total of 511 of these substances were missing RI data, requiring prediction (see below). The second list was derived from both the Arctic Monitoring and Assessment Programme's list of chemicals of emerging Arctic concern, as well as the European Chemical Agency's list of substances of very high concern.[10,11] Substances with ionizable functional groups and substances which already occurred on the first list were removed, leaving a total of 530 chemicals of concern. For this list, only 74 contaminants had literature CCS values in the aforementioned unified database,[7] while 63 had literature RI data.

Since analytes can be ionized through charge/proton transfer using APCI,[6] exact masses of the most abundant isotope for both $M^{+\cdot}$ and $[M+H]^+$ ions were calculated. We assumed that possible discrepancies in CCS values among $M^{+\cdot}$, $[M+H]^+$, and $[M-H]^-$ ions fell within measurement uncertainty. For compounds lacking literature CCS values, predictions were made for $[M+H]^+$ ions using the AllCCS2 algorithm.[12] Since alkanes evade ionization using APCI, the Fiehn RI was adopted with fatty acid methyl esters as references.[13] For both lists, experimental Fiehn RIs were collected from the MS-DIAL metabolomics MSP spectral kit, if available.[14] Kovats RIs for the remaining compounds were sourced from the NIST RI library, or otherwise predicted using a deep convolutional neural network method.[15] Kovats RIs were then converted to Fiehn RIs, and thereafter RT. Conversions among RT and RIs are described in Section C and Table S1-3 in the SI. The two suspect lists can be found in Tables S4 and S5 in the SI.

The quality of suspect list data was estimated by comparing measured and literature/model-predicted values. $MS^1$, RT, CCS, and $MS^2$ were acquired for 102 environmental contaminant standards ($1.44 < \log K_{ow} < 16.8$; $-9.31 < \log K_{aw} < 11.3$), including polycyclic aromatic hydrocarbons (PAHs), organophosphate esters (OPEs), polychlorinated biphenyls (PCBs), polybrominated diphenyl ethers (PBDEs), and other organohalogens. We further predicted RTs for all 102 of these contaminants and CCS values for a subset of 85 capable of generating $M^{+\cdot}$, $[M+H]^+$, or $[M-H]^+$ ions as base peaks using aforementioned models. These contaminants, together with their measured and predicted qualitative information, are listed in Table S6 in the SI.

**Multidimensional suspect screening.** Inspired by a previously developed approach for metabolomics,[16] a workflow with a continuous scoring system was established. This approach differs from confidence level systems (e.g., the Schymanski confidence scale) by providing continuous uncertainty/similarity information to reduce false positive results and improve identification confidence.[17,18]

Peaks were matched against suspect lists by exact mass, RT, and CCS using a custom R script (available at https://github.com/Xiaodi-Shi/4D-suspect). The error threshold for exact mass measurements was set to <5 ppm for substances with mass-to-charge >200 Da and <2 mDa for substances <200 Da. For RT and CCS, differences between measured and reference values were calculated using Equations (E) 1 and 2. A difference smaller than the high-confidence threshold ($CT_{high}$) scored 100%, while peaks with differences larger than the low-confidence threshold were excluded ($CT_{low}$). If a difference fell between $CT_{high}$ and $CT_{low}$, a score was calculated using E3.

$$\Delta RT\ (min) = RT_{measured} - RT_{reference} \quad \text{E1}$$

$$\Delta CCS\ (\%) = \frac{CCS_{measured} - CCS_{reference}}{CCS_{reference}} \times 100\% \quad \text{E2}$$

$$Score\ (\%) = \begin{cases} 100 & , \Delta RT\ or\ \Delta CCS \leq CT_{high} \\ 100 - \frac{(\Delta - CT_{high}) \times 100}{(CT_{low} - CT_{high})} & , CT_{high} < \Delta RT\ or\ \Delta CCS < CT_{low} \\ 0 & , \Delta RT\ or\ \Delta CCS \geq CT_{low} \end{cases} \quad \text{E3}$$

The thresholds were determined based on the quality of suspect lists (see discussion in the next section). Only candidates with matches in all three dimensions were retained.

$MS^1$ and $MS^2$ spectra were further checked. Observation of at least one isotope ion was required, and the geometric mean of isotopic relative intensity deviation should be lower than 5%.[19] $MS^2$ similarity scores were acquired from SIRIUS+CSI:FingerID

(version 5.8.6).[20] Since candidates were known after matches of exact mass, RT, and CCS, we specified the formula, adduct, parent ion, and InChIKey in SIRIUS. Detailed SIRIUS parameters are described in Section B of the SI. The performance of $MS^2$ similarity using SIRIUS was evaluated using 63 of 102 measured contaminants with $M^{+\cdot}$/$[M+H]^+$ ions as the base peak and at least two detected monoisotopic fragment ions in $MS^2$. Fragment ions of these 63 contaminants are provided in the SI in NIST MSP library format. The final multidimensional score was calculated using E4.

$$Score\ (\%) = W_{RT} \times Score_{RT} + W_{CCS} \times Score_{CCS} + W_{MS^2} \times Score_{MS^2} \quad \text{E4}$$

The true positive rate was independent of the assignment of weights in this study, based on testing with real sediment samples (see Figure S1 in the SI). Considering the dependence of RT on chromatographic conditions, less weight was assigned to the RT score ($W_{RT}$=0.2) than CCS and $MS^2$ scores (0.4 for both). The same weightings were previously employed in a liquid chromatography (LC)-based metabolomic workflow.[16] When the $MS^2$ score could not be estimated (e.g., < two detected monoisotopic fragment ions in $MS^2$), accurate measurement of RT and CCS becomes essential. Thus, the cutoff score was set at 60% for potential candidates. The highest-scored candidate for each suspect compound was retained.

**Workflow validation.** The workflow was validated in two types of sediment (both measured in triplicate) by assessing the true positive identification rate for 37 contaminants (Table S6 in the SI) which occurred on our suspect lists and for which standards were available. The first sediment was a NIST standard reference material

(SRM; 1941b-Organics in Marine Sediment), while the second was a fortified surface (0-2 cm) sediment collected from a reference site (58.26º N,16.91º E) in the Baltic Sea in January 2023.[21] The NIST material was used as-received while the fortified sediment was prepared by sieving (mesh size 1 mm), followed by addition of about 1 ng of each contaminant. Samples were extracted three times by accelerated solvent extraction (ASE 350; Dionex, U.S.A.) using 20 mL of acetone/n-hexane (1:1 v/v) per cycle, following previously described procedures (for further details, see Section D of the SI).[8] Instrumental analysis and data processing were carried out as described above.

## RESULTS AND DISCUSSION

**Performance of model predictions for suspect lists.** Among 102 measured contaminants, 34 already had literature CCS values in our suspect lists, offering an opportunity to evaluate the accuracy of our measured values. Previous interlaboratory and interplatform comparisons reported that CCS relative deviations tend to be within ±2%.[7,22-24] In the present work, relative deviations between measured and experimentally-derived CCS values fell within ±2% for 67.6% of substances, and within ±3% for 82.3% (Figure 1A). Based on these results, high- and low-confidence thresholds for literature CCS values were set at ±2% and ±3%, respectively. For the remaining 68 substances, experimentally determined CCS values are reported here for the first time.

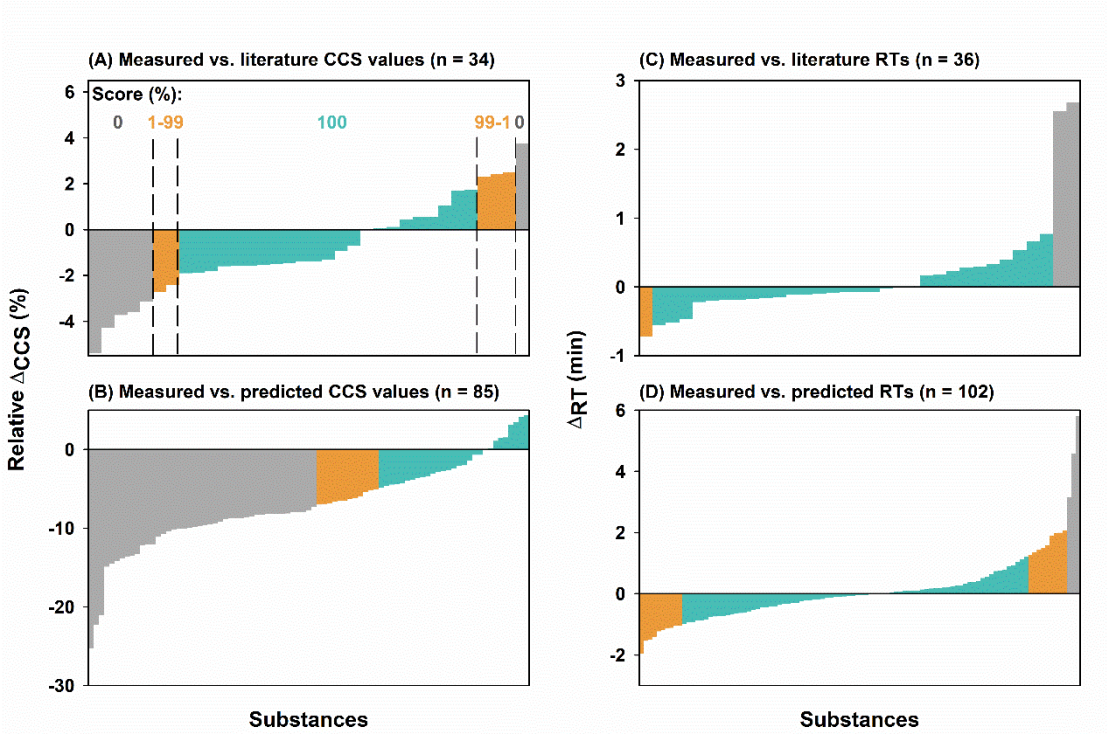


**Figure 1.** Distribution of relative deviations between measured collision cross section (CCS) values with either literature (A) or predicted (B) values; distribution of differences between measured retention times (RTs) with either literature (C) or predicted (D) values. Using Panel A as an example, differences within high-confidence thresholds (denoted by green bars) score 100%, while differences outside low-confidence thresholds (denoted by grey bars) score 0%. A continuous score was calculated for differences between high- and low-confidence thresholds (denoted by orange bars). n is the number of substances.

The comparison between our measured and predicted CCS values for 85 contaminants capable of generating $M^{+\cdot}$, $[M+H]^+$, or $[M-H]^+$ ions as base peaks showed an average relative deviation (±standard deviation [SD]) of -7.03% (±5.42%), indicating an overprediction of CCS values by the ALLCCS2 model. This considerable discrepancy is attributed to the fact that most compounds used in the model's training set are non-halogenated endogenous metabolites which tend to have larger CCS values than halogenated substances.[12,25] All relative deviations in measured CCS values among available isomers fell within 5%. To avoid misidentification at the isomeric level, high- and low-confidence thresholds for predicted CCS values were set at ±5% and ±7% covering 34.1% and 48.2% of 85 measured contaminants, respectively (Figure 1B).

In contrast to CCS, uncertainties associated with RT predictions (mean ± SD of 0.086 ± 1.13 min, n=102) are comparable to those of RTs converted from literature RI values (mean ± SD of 0.15 ± 0.69 min, n=36; Figure 1C-D). This resulted from the similarity between our measured contaminants and compounds for model training.[15] For RTs from both sources, mean ± SD and mean ± 2 × SD were selected as high- and low-confidence thresholds, respectively.

The performance of SIRIUS for HOCs was evaluated using 63 of 102 measured contaminants with $M^{+\cdot}$/$[M+H]^+$ ions as the base peak and at least two detected monoisotopic fragment ions in $MS^2$. The mean ± SD of SIRIUS similarities were 72.43 ± 18.0 %. (see Table S6 in the SI for detailed scores). Although this model is mainly trained on data acquired using electrospray ionization,[20] the relatively high scores observed indicate that the mechanism of collision induced dissociation could be independent of ionization method.

**Workflow validation.** The number of compound hits decreased as more dimensions were added to the screening (Figure 2). There were 63 and 66 hits in the fortified sediment and SRM 1941b, respectively, with all exact mass, RT, and CCS matched. These numbers are 36.3% and 40% lower than those obtained with only exact mass and RT matched for the fortified sediment and SRM1941b, respectively. This indicates that the analytical space for potential candidates can be effectively constrained using CCS as an additional dimension.

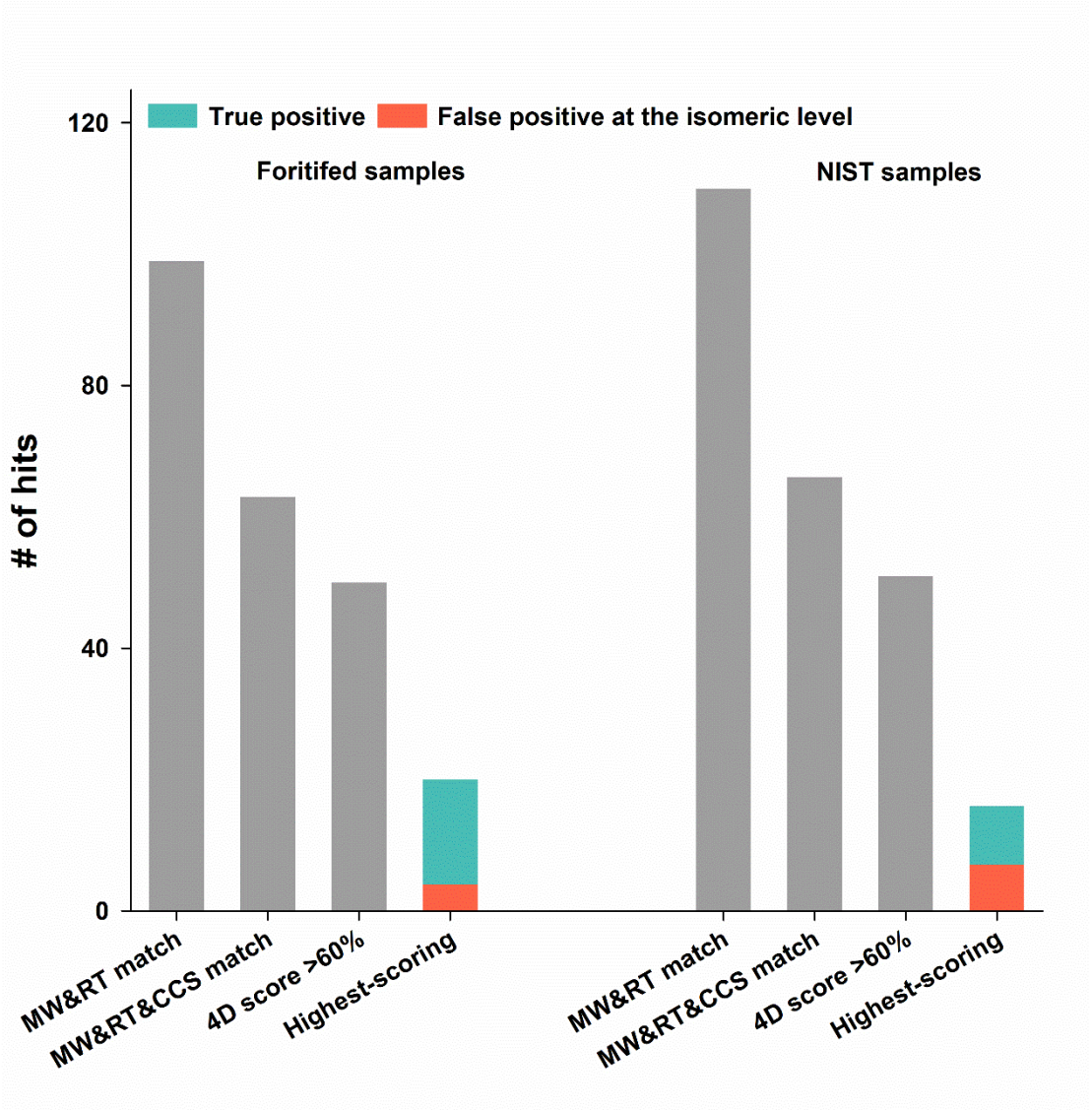


**Figure 2.** Number of hits in fortified- and NIST samples at different steps in the suspect screening workflow (from left to right): hits with molecular weight (MW) and retention time (RT) match; MW, RT, and collision cross section (CCS) match; four-dimensional (4D) score over 60%; and the highest score.

After checking mass spectra, 50 candidates in the fortified sediment and 51 candidates in SRM 1941b remained (i.e. multidimensional scores >60%; Figure 2). According to the Schymanski confidence scale, these candidates would be classified as level 2/3, indicating a large fraction of false positive results.[17,18] Our continuous scoring system can aid in further narrowing down the number of candidates. Finally, the highest-scoring candidates for each suspect compound were retained (19 in the fortified

sediment and 14 in SRM 1941b). These hits included PAHs, PCBs, PBDEs, OPEs, hexachlorobenzene, and 1,2-bis(2,4,6-tribromophenoxy)ethane. Detailed scores for each compound are listed in the Table S7 in the SI. The true positive rates were 78.9% and 64.3% for the fortified and standard samples, respectively (Figure 2). Notably, all false positives were isomers of the correct compounds. These results suggest that the combination of the exact mass of the molecular ion, isotopic distribution, and fragment ions can effectively determine the elemental composition, particularly for halogenated compounds, while CCS matching further constrains the general structure.

**Perspectives.** Based on analytical data acquired by GC-APCI-IM-HRMS, a suspect screening workflow for HOCs constrained by $MS^1$, RT, CCS, and $MS^2$, together with a continuous scoring system, was established for the first time. True positive rates of 78.9% and 64.3% for the fortified sediment and SRM 1941b were achieved, respectively, with misidentification only at the isomeric level. CCS of (quasi-)molecular ion is a confirmatory dimension with high reproducibility to improve identification confidence. However, since conventional EI for GC-based characterization hampers formation of the molecular ions, prior experimental CCS values were acquired mostly for compounds suitable for LC measurement with soft ionization. In our suspect lists, 1,134 compounds had literature CCS values, representing only 28% of organic pollutants in the unified CCS database, and over 20 times fewer than the number of compounds in the METLIN-CCS database.[7,26] Consequently, current CCS prediction models, primarily trained on non-halogenated endogenous metabolites, displayed considerable error (mean ± SD: -7.23% ± 5.32%) when predicting CCS for HOCs (which are mainly halogenated) in this study. Harnessing molecular ions using APCI presents opportunities to enrich CCS databases for HOCs and to extend the applicable chemical

space of current models from polar to non-polar compounds. This advancement is crucial for keeping analytical techniques aligned with the introduction of emerging chemicals with diverse properties.

## ASSOCIATED CONTENT

### Supporting Information

Additional information as noted in the text is available.

Instrumental method (Section A); software parameters (Section B); conversion between RTs and RIs (Section C); regressions among RTs and RIs (Table S1); RTs and RIs of fatty acid methyl esters (Table S2); measured RTs of alkanes (Table S3); suspect list of GC-amenable chemicals with experimentally-derived CCS values (Table S4); suspect list of chemicals of concern (Table S5); qualitative information of reference standards (Table S6); true positive rates using different weights (Figure S1); sample preparation (Section D); highest-scoring candidates in sediment samples (Table S7) (XLSX).

$MS^2$ library (MSP).

R scripts for exact mass, RT, CCS matching and format converting can be found at https://github.com/Xiaodi-Shi/4D-suspect.

## AUTHOR INFORMATION

### Corresponding Author

**Xiaodi Shi** - Department of Environmental Science, Stockholm University, Stockholm 10691, Sweden; ORCID: 0009-0008-4062-4009; E-mail: xiaodi.shi@aces.su.se.

## Notes

The authors declare no competing financial interest.


## ACKNOWLEDGEMENTS

We thank Gastón Alurralde and Elena Gorokhova (both at Department of Environmental Science, Stockholm University) for providing sediment samples. This research was supported by a Marie Sklodowska-Curie postdoctoral fellowship under Horizon Europe (Grant agreement number: 101150779), Ymer-80 foundation, and faculty funding of Department of Environmental Science, Stockholm University.


## REFERENCE


(1) Wang, Z.; Walker, G. W.; Muir, D. C. G.; Nagatani-Yoshida, K. Toward a global understanding of chemical pollution: A first comprehensive analysis of regulatory industrial chemical inventories. *Environ. Sci. Technol.* **2020**, *54*, 2575−2584.

(2) Muir, D.; Getzinger, G.; McBride, M.; Ferguson, P. How many chemicals in commerce have been analyzed in environmental media? A 50 year bibliometric analysis. *Environ. Sci. Technol.* **2023**, *57*, 9119−9129.

(3) Hollender, J.; Schymanski, E.; Ahrens, L.; Alygizakis, N.; Béen, F.; Bijlsma, L.; Brunner, A.; Celma, A.; Fildier, A.; Fu, Q.; Gago-Ferrero, P.; Gil-Solsona, R.; Haglund, P.; Hansen, M.; Kaserzon, S.; Kruve, A.; Lamoree, M.; Margoum, C.; Meijer, J.; Merel, S.; Rauert, C.; Rostkowski, P.; Samanipour, S.; Schulze, B.; Schulze, T.; Singh, R.; Slobodnik, J.; Steininger-Mairinger, T.; Thomaidis, N.; Togola, A.; Vorkamp, K.;

315 Vulliet, E.; Zhu, L.; Krauss, M. NORMAN guidance on suspect and non-target
316 screening in environmental monitoring. *Environ. Sci. Eur.* **2023**, *35*, 75.
317 (4) Phillips, K.; Yau, A.; Favela, K.; Isaacs, K.; McEachran, A.; Grulke, C.; Richard, A.;
318 Williams, A.; Sobus, J.; Thomas, R.; Wambaugh, J. Suspect screening analysis of
319 chemicals in consumer products. *Environ. Sci. Technol.* **2018**, *52*, 3125−3135.
320 (5) Schymanski, E.; Gallampois, C.; Krauss, M.; Meringer, M.; Neumann, S.; Schulze,
321 T.; Wolf, S.; Brack, W. Consensus structure elucidation combining GC/EI-MS, structure
322 generation, and calculated properties. *Anal. Chem.* **2012**, *84*, 3287−3295.
323 (6) Ayala-Cabrera, J.; Montero, L.; Meckelmann, S.; Uteschil, F.; Schmitz, O. Review
324 on atmospheric pressure ionization sources for gas chromatography-mass spectrometry.
325 Part I: Current ion source developments and improvements in ionization strategies.
326 *Anal. Chim. Acta.* **2023**, *1238*, 340353.
327 (7) Song, X.; Canellas, E.; Dreolin, N.; Goshawk, J.; Lv, M.; Qu, G.; Nerin, C.; Jiang,
328 G. Application of ion mobility spectrometry and the derived collision cross section in
329 the analysis of environmental organic micropollutants. *Environ. Sci. Technol.* **2023**, *57*,
330 21485–21502.
331 (8) Shi, X.; Langberg, H.; Sobek, A.; Benskin, J. Exploiting molecular ions for
332 screening hydrophobic contaminants in sediments using gas chromatography-
333 atmospheric pressure chemical ionization-ion mobility mass spectrometry. *ChemRxiv.*
334 **2024**, doi:10.26434/chemrxiv-2024-ft9cl.
335 (9) Mohammed Taha, H.; Aalizadeh, R.; Alygizakis, N.; Antignac, J.; Arp, H.; Bade, R.;
336 Baker, N.; Belova, L.; Bijlsma, L.; Bolton, E.; Brack, W.; Celma, A.; Chen, W.; Cheng,

T.; Chirsir, P.; Čirka, Ľ.; D'Agostino, L.; Djoumbou Feunang, Y.; Dulio, V.; Fischer, S.; Gago-Ferrero, P.; Galani, A.; Geueke, B.; Głowacka, N.; Glüge, J.; Groh, K.; Grosse, S.; Haglund, P.; Hakkinen, P.; Hale, S.; Hernandez, F.; Janssen, E.; Jonkers, T.; Kiefer, K.; Kirchner, M.; Koschorreck, J.; Krauss, M.; Krier, J.; Lamoree, M.; Letzel, M.; Letzel, T.; Li, Q.; Little, J.; Liu, Y.; Lunderberg, D.; Martin, J.; McEachran, A.; McLean, J.; Meier, C.; Meijer, J.; Menger, F.; Merino, C.; Muncke, J.; Muschket, M.; Neumann, M.; Neveu, V.; Ng, K.; Oberacher, H.; O'Brien, J.; Oswald, P.; Oswaldova, M.; Picache, J.; Postigo, C.; Ramirez, N.; Reemtsma, T.; Renaud, J.; Rostkowski, P.; Rüdel, H.; Salek, R.; Samanipour, S.; Scheringer, M.; Schliebner, I.; Schulz, W.; Schulze, T.; Sengl, M.; Shoemaker, B.; Sims, K.; Singer, H.; Singh, R.; Sumarah, M.; Thiessen, P.; Thomas, K.; Torres, S.; Trier, X.; van Wezel, A.; Vermeulen, R.; Vlaanderen, J.; von der Ohe, P.; Wang, Z.; Williams, A.; Willighagen, E.; Wishart, D.; Zhang, J.; Thomaidis, N.; Hollender, J.; Slobodnik, J.; Schymanski, E. The NORMAN Suspect List Exchange (NORMAN-SLE): Facilitating European and worldwide collaboration on suspect screening in high resolution mass spectrometry. *Environ. Sci. Eur.* **2022**, *34*, 104.

(10) Candidate List of substances of very high concern for Authorisation, European Chemical Agency. https://echa.europa.eu/candidate-list-table.

(11) Reppas-Chrysovitsinos, E.; Sobek, A.; MacLeod, M. Screening-level exposure-based prioritization to identify potential POPs, vPvBs and planetary boundary threats among Arctic contaminants. *Emerg. Contam.* **2017**, *3*, 85–94.

(12) Zhang, H.; Luo, M.; Wang, H.; Ren, F.; Yin, Y.; Zhu, Z. AllCCS2: Curation of ion mobility collision cross-section atlas for small molecules using comprehensive

molecular representations. *Anal. Chem.* **2023**, *95*, 13913–13921.

(13) Kind, T.; Wohlgemuth, G.; Lee, D.; Lu, Y.; Palazoglu, M.; Shahbaz, S.; Fiehn, O. FiehnLib: Mass spectral and retention index libraries for metabolomics based on quadrupole and time-of-flight gas chromatography/mass Spectrometry. *Anal. Chem.* **2009**, 81, 10038–10048.

(14) Lai, Z.; Tsugawa, H.; Wohlgemuth, G.; Mehta, S.; Mueller, M.; Zheng, Y.; Ogiwara, A.; Meissen, J.; Showalter, M.; Takeuchi, K.; Kind, T.; Beal, P.; Arita, M.; Fiehn, O. Identifying metabolites by integrating metabolome databases with mass spectrometry cheminformatics. *Nat. Methods*. **2018**, 15, 53–56.

(15) Matyushin, D.; Sholokhova, A.; Buryak, A. A deep convolutional neural network for the estimation of gas chromatographic retention indices. *J. Chromatogr. A.* **2019**, 1607, 460395.

(16) Zhou, Z.; Luo, M.; Chen, X.; Yin, Y.; Xiong, X.; Wang, R.; Zhu, Z. Ion mobility collision cross-section atlas for known and unknown metabolite annotation in untargeted metabolomics. *Nat. Commun.* **2020**, *11*, 1–13.

(17) Celma, A.; Sancho, J.; Schymanski, E.; Fabregat-Safont, D.; Ibáñez, M.; Goshawk, J.; Barknowitz, G.; Hernández, F.; Bijlsma, L. Improving target and suspect screening high-resolution mass spectrometry workflows in environmental analysis by ion mobility separation. *Environ. Sci. Technol.* **2020**, *54*, 15120−15131.

(18) Schymanski, E.; Jeon, J.; Gulde, R.; Fenner, K.; Ruff, M.; Singer, H.; Hollender, J. Identifying small molecules via high resolution mass spectrometry: Communicating confidence. *Environ. Sci. Technol.* **2014**, *48*, 2097−2098.

(19) Kind, T.; Fiehn, O. Seven Golden Rules for heuristic filtering of molecular formulas obtained by accurate mass spectrometry. *BMC Bioinformatics*. **2007**, *8*, 105.

(20) Dührkop, K.; Fleischauer, M.; Ludwig, M.; Aksenov, A.; Melnik, A.; Meusel, M.; Dorrestein, P.; Rousu, J.; Böcker, S. SIRIUS 4: A rapid tool for turning tandem mass spectra into metabolite structure information. *Nat. Methods*. **2019**, *16*, 299–302.

(21) Blomqvist, S.; Lundgren, L. A benthic sled for sampling soft bottoms. *Helgoländer Meeresunters.* **1996**, *50*, 453–456.

(22) Hinnenkamp, V.; Klein, J.; Meckelmann, S.; Balsaa, P.; Schmidt, T.; Schmitz, O. Comparison of CCS values determined by traveling wave ion mobility mass spectrometry and drift tube ion mobility mass spectrometry. *Anal. Chem.* **2018**, *90*, 12042–12050.

(23) Stow, S.; Causon, T.; Zheng, X.; Kurulugama, R.; Mairinger, T.; May, J.; Rennie, E.; Baker, E.; Smith, R.; McLean, J.; Hann, S.; Fjeldsted, J. An interlaboratory evaluation of drift tube ion mobility–mass spectrometry collision cross section measurements. *Anal. Chem.* **2017**, *89*, 9048–9055.

(24) Izquierdo-Sandoval, D.; Fabregat-Safont, D.; Lacalle-Bergeron, L.; Sancho, J.; Hernández, F.; Portoles, T. Benefits of ion mobility separation in GC-APCI-HRMS screening: From the construction of a CCS library to the application to real-world samples. *Anal. Chem.* **2022**, *94*, 9040–9047.

(25) Macneil, A.; Li, X.; Amiri, R.; Muir, D.; Simpson, A.; Simpson, M.; Dorman, F.; Jobst, K. Gas chromatography-(cyclic) ion mobility mass spectrometry: A novel platform for the discovery of unknown per-/polyfluoroalkyl substances. *Anal. Chem.*

**2022**, *94*, 11096−11103.

(26) Baker, E.; Hoang, C.; Uritboonthai, W.; Heyman, H.; Pratt, B.; MacCoss, M.; MacLean, B.; Plumb, R.; Aisporna, A.; Siuzdak, G. METLIN-CCS: an ion mobility spectrometry collision cross section database. *Nat. Methods*. **2023**, *20*, 1836–1837.